Dynamics of Linear and Star Poly(oxypropylene) Studied by Dielectric Spectroscopy and Rheology

Taco Nicolai*

Chimie et Physique des Matériaux Polymères, UMR CNRS, Université du Maine, 72085 Le Mans Cedex 9, France

George Floudas

Foundation for Research and Technology-Hellas (FORTH), Institute of Electronic Structure and Laser, P.O. Box 1527, 711 10 Heraklion, Crete, Greece

Received September 23, 1997; Revised Manuscript Received January 28, 1998

ABSTRACT: We give a quantitative comparison of dielectric and viscoelastic relaxation of identical poly(oxypropylene) (POP) diols and triols with molar masses in the range 260−11 000 g/mol. The segmental relaxation probed in dielectric spectroscopy (DS) is slower by a factor of 8 ± 1, while the conformational relaxation of the whole chain is faster by a factor of 2.5 ± 0.5. The molar mass dependence of the conformational relaxation is close to the prediction of the Rouse model. POP diol with molar mass larger than 4000 g/L shows the influence of entanglement. A "fast" β-relaxation with Arrhenius temperature dependence is observed in all samples by DS. Measurements made on very low molar mass samples show that hydroxyl end groups are involved in this relaxation.

Introduction

The dynamical properties of bulk poly(oxypropylene) diols and triols have been extensively studied in the past by a number of techniques (e.g., refs 1−16). Four relaxation processes have been reported: the segmental (or α) relaxation, which characterizes the glass−rubber transition; the so-called normal mode, which characterizes the conformational relaxation of the polymer backbone; a fast β-relaxation of the system in the glassy state; and an even faster ill-defined γ-relaxation. All these modes can be observed by dielectric spectroscopy (DS) because POP contains both dipoles parallel and perpendicular to the chain backbone, giving rise to long- and short-range motions, respectively.[3] The temperature (T) dependence of the first two modes can be described by the empirical Vogel−Fulcher−Tammann (VFT) equation (see eq 2) while the β-relaxation has an Arrhenius temperature dependence. An interesting and still unexplained feature is that the temperature dependence of the segmental and conformational relaxation is not the same, at least for temperatures close to the glass transition temperature (T_g). This feature is observed for many polymeric systems (e.g., refs 17 and 18) and an attempt has been made to explain it in terms of the coupling model introduced by Ngai and coworkers.[19,20] The molar mass dependence of the normal mode was found to be stronger than predicted by the Rouse model, which has been attributed to the effect of hydrogen bonding. However, one should be aware that these conclusions were based on samples with a limited range of molar masses that were commercially available at the time.

Recently, a novel synthesis method has made commercially available POP of higher molar mass (up to 11 000 g/mol) with well-defined functionality. On the basis of this development, we can study the molar mass dependence of the normal mode over a wider range and investigate the effect of entanglements. It will be shown here that the deviation from the Rouse model reported in the literature is only apparent and is due to an underestimation of the molar mass of the larger samples used in these studies. Furthermore, we provide the first quantitative comparison of mechanic and dielectric measurements on identical POP samples covering both segmental and conformational relaxation. Finally, we study the finite size effects on the local segmental and glassy modes by investigating a number of very low molar mass samples.

Experimental Section

Samples. We have investigated a series of POP diols with molar masses between 430 and 11 000 g/mol and POP triols between 260 and 6000 g/mol. The samples D4200, D8200, D12200, and T6300 with trade name "Acclaim" were kindly provided by Arco and were synthesized using a new method. This method yields much better functionality for the high molar mass samples necessary for the present investigation. The samples T720 and T2500 were also provided by Arco, and the other samples were purchased from Aldrich. All samples were characterized by size exclusion chromatography (SEC) and had a polydispersity index (M_w/M_n) less than 1.2 except for T4100 and D3000. These samples contained a lower molar mass fraction of about 5%, thus increasing the polydispersity index to slightly above 1.2. The number average molar mass M_n was calculated from the hydroxyl content by assuming full functionality and is given in Table 1. All samples were dried under vacuum before use.

Rheology. Dynamic shear measurements were made on a Rheometrics RDA II dynamic spectrometer using parallel-plate geometry at temperatures between 200 and 340 K. The so-called hold mode was used where the gap is corrected for temperature variations of the sample volume. The plate size (diameters 50, 25, 8, and 4 mm) and the imposed deformation (0.2−20%) were adjusted to obtain an accurate torque response while remaining in the linear regime. The shear modulus could be measured in the range $10-10^9$ Pa. We were able to measure very large moduli by using a relatively large sample thickness (2−2.5 mm) in combination with a small plate size. The range of frequencies used was $10^{-2}-10^2$ rad/s. Temper-

S0024-9297(97)01406-X CCC: $15.00 © 1998 American Chemical Society
Published on Web 04/04/1998

Table 1. Sample Characteristics

sample	M_n (kg/mol)	T_g (K)	$\log(\tau_0/s)^a$	τ_{vis}/τ_{DS}
D425	0.43	200		
D1000	1.01	202	−11.7	
D2000	2.00	203	−11.1	2.1
D3000	2.95	203	−10.6	2.8
D4200	4.05	204.5	−10.1	2.4
D8200	7.65	204.5	−9.8	3.0
D12200	11.0	205	−9.3	2.4
T260	0.26	217		
T720	0.72	211		
T2500	2.54	206	−11.3	2.0
T4100	4.16	204	−10.6	1.4
T6300	6.15	206	−10.2	3.0

[a] Values obtained from VFT fits to the DS results.

atures were measured using a thermocouple close to the lower plate. The temperature was stable within ±0.2 K over the whole range used in this study (200−350 K).

Dielectric Spectroscopy. Measurements of the complex dielectric function were made with a Novocontrol BDS-S system composed of a frequency response analyzer (Solartron Schlumberger FRA 1260) and a broad band dielectric converter with an active sample cell. The latter contains six reference capacitors ranging from 25 to 100 pF. Measurements were made in the frequency range from 2×10^{-4} to 3×10^{6} using a combination of three capacitors in the active sample cell. The samples were kept between two gold-plated stainles steel plates of 30 mm in diameter with a separation of about 100 μm. The sample cell was set in the cryostat, and the sample temperature was controlled between 143 and 333 K and measured with a PT100 sensor in the lower plate of the sample capacitor with an accuracy of ±0.1 K. Some typical dielectric measurements are shown in Figure 1.

Results and Discussion

I. Dielectric Spectroscopy. Four well-separated processes contribute to the dielectric relaxation spectrum within the temperature and frequency range investigated. Notwithstanding the broad frequency range employed, which extends over 10 decades, the different length scales reflecting local and global motions and the associated activation energies preclude a visual inspection of all modes at a single temperature. Starting from high temperatures, we observe the so-called normal mode characterizing chain backbone conformational relaxation, the segmental mode, and two modes below the glass−rubber relaxation that we refer to as the "slow" and "fast" glassy modes. The upturn of ϵ'' at low frequencies is due to the conductivity. At even lower temperatures and at high frequencies there is an indication of another glassy mode, which, however, relaxes outside the experimental window. Some typical spectra at temperatures above and below T_g are shown in Figure 1.

To analyze the isothermal dielectric loss and storage, we have used the empirical Havriliak−Negami (HN) function:

$$\epsilon^*(\omega) = \epsilon_\infty + \frac{\epsilon_0 - \epsilon_\infty}{[1 + (i\omega\tau_{HN})^\alpha]^\gamma} \qquad (1)$$

where $\omega = 2\pi f$ is the angular frequency and $\Delta\epsilon = \epsilon_0 - \epsilon_\infty$ is the relaxation strength, with ϵ_∞ and ϵ_0 being, respectively, the high- and low-frequency limit of the process under investigation. The parameters α and γ describe, respectively, the symmetrical and asymmetrical broadening of the distribution of relaxation times. In a $\log(\epsilon'')$ vs $\log(f)$ plot, α and $\alpha\gamma$ give the low- and high-frequency slopes of the relaxation function, respectively. The solid lines in Figure 1a,b represent nonlinear least-squares fits to the sum of two HN functions. We did simultaneous fits of the loss and storage data.

We start our discussion from the glassy modes (see Figure 1c,d). The shape parameters assume the values $\alpha = 0.25$, $\gamma = 1$ and $\alpha = 0.6$, $\gamma = 1$ for the "fast" and "slow" processes, respectively. Although the strong overlap with adjacent processes results in considerable uncertainty in the fit parameters, superposition of the modes obtained at different temperatures showed that the shape of these modes has no significant temperature dependence. Furthermore, superposition of the modes obtained from different samples showed little dependence of the shape on the molar mass. The temperature corrected strength ($T\Delta\epsilon$) of the "fast" glassy mode was found to increase almost linearly with increasing temperature from 25 to about 100 in the range 133−193 K. In the framework of the free volume fluctuations existing in glasses,[21] the increasing strength can be understood in terms of an increasing number of dipoles involved in the relaxation.

The temperature dependence of the peak frequency shown in Figure 2 shows the expected Arrhenius dependence with apparent activation energies 32 ± 1 and 46 ± 4 kJ/mol for the "fast" and "slow" glassy mode, respectively, independent of the molar mass. It is worth mentioning that the activation energy of the "fast" mode is within experimental error the same as that of the single high-frequency process observed in an earlier study utilizing Brillouin spectroscopy.[14] Moreover, the absolute values are of the same order of magnitude as the DS data extrapolated to high frequency.

The "fast" glassy mode can be identified with the β-relaxation reported by Johari[15] on a POP of 4000 g/mol. The slower process with the steeper temperature dependence has not been reported earlier. The amplitude of this mode depends on the degree of exposure to moisture, and we believe that it reflects the dynamics of traces of water that survived the drying procedure.

At frequencies below the normal mode there is an upturn in the dielectric loss that is caused by the conductivity contribution (see Figure 1b). This extra contribution was fitted according to $\epsilon'' = (\sigma_{dc}/\epsilon_0)\omega^{-1}$, where σ_{dc} is the dc conductivity and ϵ_0 (=8.854 pF/m) is the permittivity of free space. The solid lines through the data points of Figures 1a,b represent nonlinear least-squares fits to the sum of two HN functions plus the conductivity term in the case of the loss data. An alternative analysis method is to use the so-called generalized exponential (GEX) relaxation time distribution, which can be chosen to be equivalent to a stretched exponential relaxation in the time domain.[22] Fits to stretched exponentials were equivalent with fits to HN functions for the segmental and normal modes. However, stretched exponentials were less successful in describing the glassy modes.

A superposition of the modes at different temperatures shows that the shape of each relaxation process is independent of the temperature except for the sample T260. The stretched exponent that characterizes the segmental relaxation is 0.53 for the high molar mass samples and increases weakly with decreasing molar mass to 0.56 for D425. These values are compatible with the value reported earlier for a POP diol with M = 4000 g/L.[15] The normal mode is narrow at low molar mass, but broadens toward the higher frequencies with

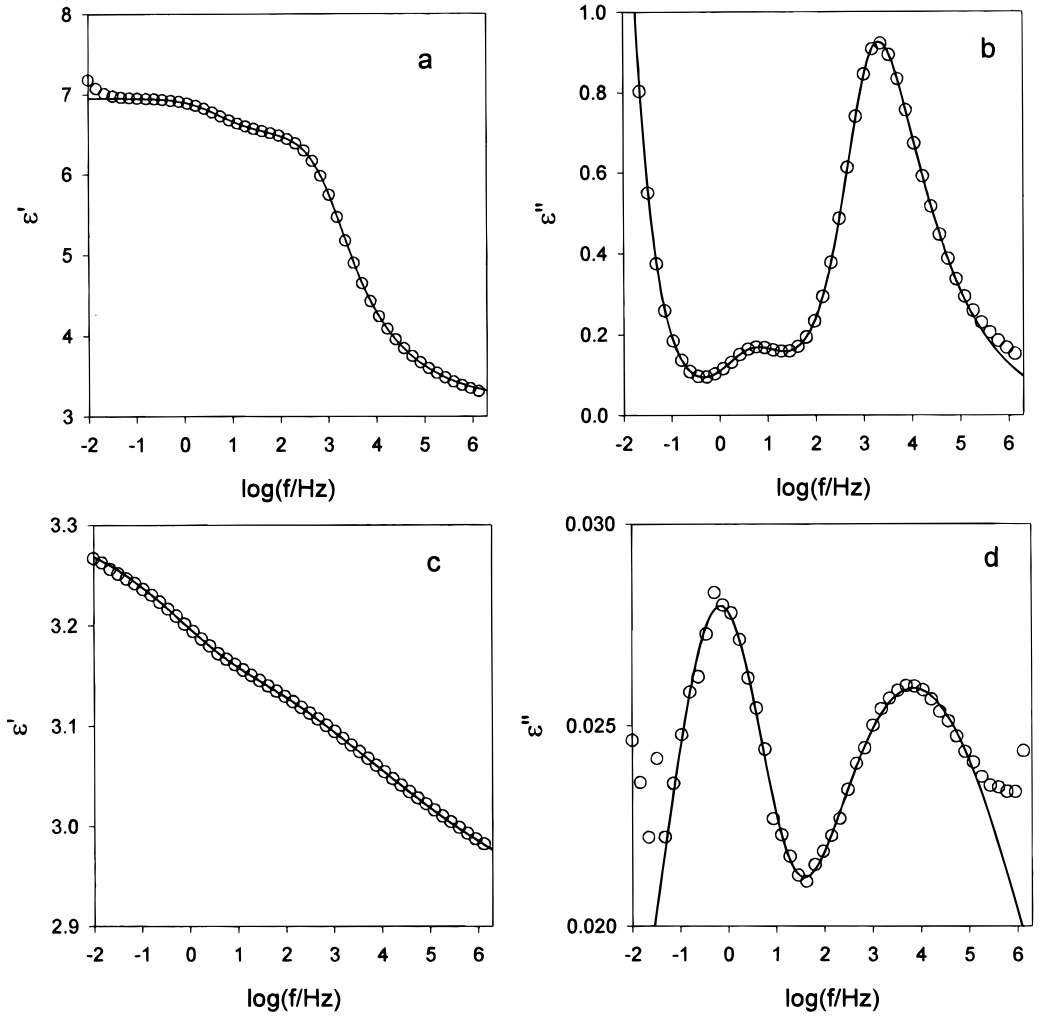

Figure 1. Frequency dependence of the storage (a, c) and loss (b, d) dielectric permittivity of sample D4200 at 218K (a, b) and 173K (c, d). The solid lines represent fits to the sum of two HN functions. In the case of the loss dielectric permittivity at 218 K (b), the conductivity term (see text) was included in the fit.

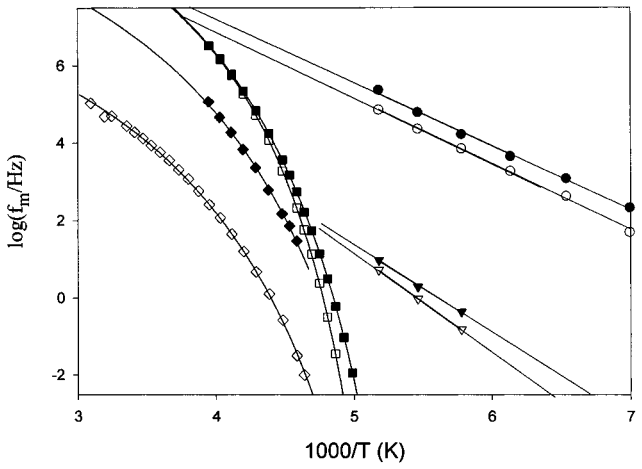

Figure 2. Arrhenius plot of the frequency corresponding to the maximum loss dielectric permittivity for the four modes resolved in the present study. For clarity, only the results of two samples are shown: D1000 (filled symbols) and D12200 (open symbols). Solid lines represent fits of the VFT equation to the segmental (squares) and the normal (diamonds) mode and linear least-squares fits to the two glassy modes (see text).

increasing molar mass. The stretched exponent decreases with increasing molar mass from 0.7 to 0.5. In all cases, the peak is broader than expected from the Rouse model.

The temperature dependence of the peak frequency (f_m) for the two modes is shown in Figure 2 together with that of the two glassy modes. For clarity, we show in Figure 2 only the results of the largest (D12200) and smallest (D1000) sample where all four modes are well separated. The results of all other samples with intermediate molar mass lie in between. The molar mass dependence of the segmental mode is small in this range. Finite size effects for even smaller samples are more marked and will be discussed below. The solid lines through the data are fits to the Vogel−Fulcher−Tammann (VFT) equation:

$$\log(\tau) = \log(\tau_0) + \frac{B}{(T - T_0)} \qquad (2)$$

with $\tau = 1/(2\pi f_m)$. Here, $\log(\tau_0)$ is the limiting value at high temperature, B is the apparent activation energy, and T_0 is the "ideal" glass transition temperature. These parameters will be discussed in detail below.

The temperature-corrected dielectric strength of the segmental mode was found to increase with decreasing molar mass but became constant at high molar mass ($M > 4000$ g/mol) where end effects can be neglected: $T\Delta\epsilon = 720 \pm 20$. The dielectric strength of the normal mode was independent of the molar mass: $T\Delta\epsilon = 110 \pm 20$. The dielectric strength of the latter is related to

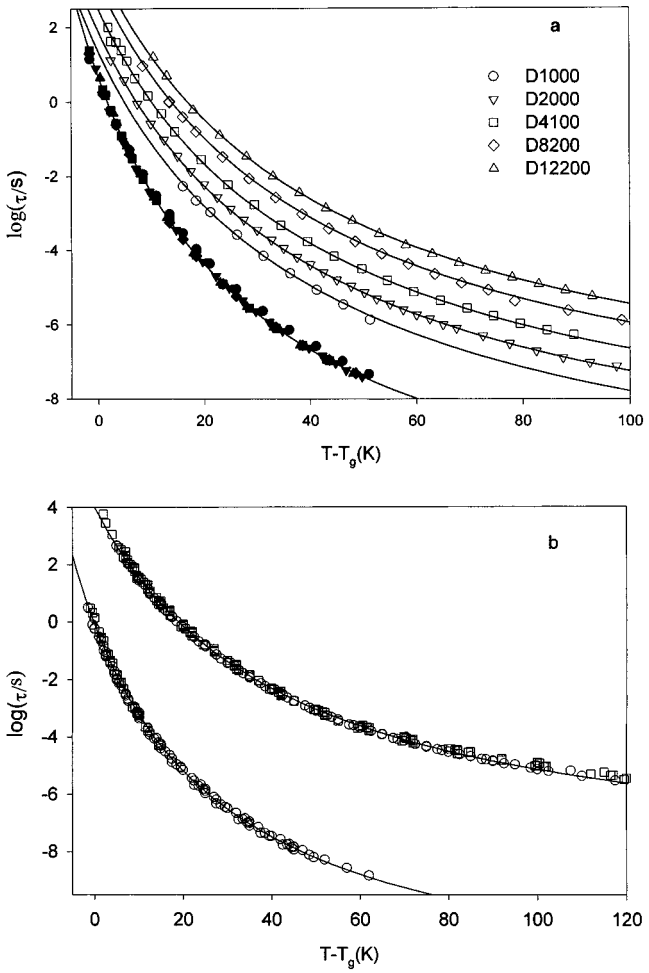

Figure 3. (a) Temperature dependence of the characteristic relaxation times ($\tau = 1/(2\pi f_m)$) of the segmental (filled symbols) and normal (open symbols) modes obtained on POP diols with different molar masses indicated in the figure. The solid lines represent fits of the VFT equation. (b) Superposition of all DS (circles) and shear modulus (squares) measurements made on POP diols and triols of different molar masses. The superposition was obtained by vertical shifts taking the shear modulus results of D12200 as the reference. The shift factors were taken as the differences in the values of log(τ_0) given in Table 1.

the mean square end-to-end distance ($\sqrt{\langle r^2 \rangle}$):[23]

$$\Delta\epsilon = \frac{4\pi\rho N_a \mu^2}{3kT}\frac{\langle r^2\rangle}{M} \qquad (3)$$

Here k is Boltzmann's constant, ρ is the density, N_a is Avogadro's constant, and μ is the dipole moment per unit contour length. $\Delta\epsilon$ is independent of the molar mass as in the melt $M = C_\infty\langle r^2\rangle$, where C_∞ is the so-called characteristic ratio. Using $C_\infty = 0.075$ mol·g^{-1}·nm^{-2} and $\rho = 0.94$ g/cm^3, we calculate a dipole moment of 0.16 D per repeat unit. This value is only slightly smaller than an earlier estimate of 0.18 D, which was based on $\Delta\epsilon'$ through the transition rather than the integrated intensity.[3]

In Figure 3 we show the characteristic relaxation times of the segmental and normal modes of a number of different POP diols as a function of $T - T_g$ where T_g is defined as the temperature where the maximum loss shear loss modulus is at 1 rad/s (see Table 1). Plotted in this way the temperature dependence of the segmental relaxation is independent of the molar mass for M > 1000 g/mol. The solid lines are again fits to the VFT, eq 2. For the segmental mode we obtained the following VFT parameters: log(τ_0/s) = 12.8, B = 445 K, and $T_g - T_0$ = 33.0 K. For all samples the temperature dependence of the normal mode could be superimposed by a simple vertical shift. This is shown in Figure 3b, where all data including those obtained on POP triols are superimposed on the results of D12200. This means that we can use the same VFT parameters to describe all samples: B = 550 K and $T_g - T_0$ = 42.2 K. Of course, log(τ_0) depends on the molar mass and the values are summarized in Table 1.

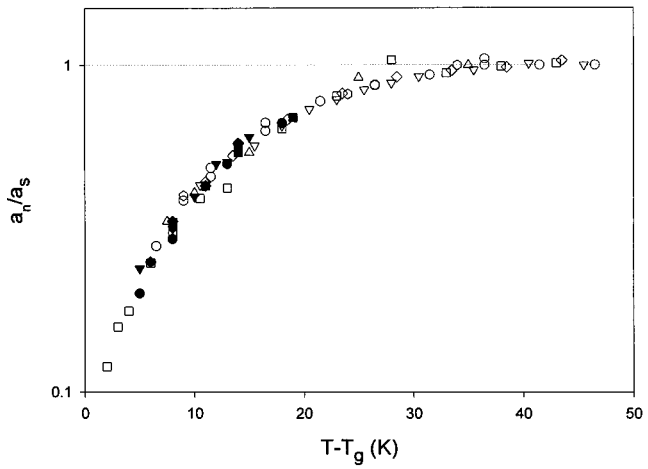

Figure 4. Temperature dependence of the ratio of the shift factors used in the time− temperature superposition of the normal and the segmental modes. Open symbols represent DS results on POP diols and triols with different molar masses, while filled symbols represent shear modulus results.

It is clear from the different values of B and $T_g - T_0$ that the segmental and normal modes do not have the same temperature dependence. To show this effect more clearly, we have plotted in Figure 4 the ratio of shift factors of the segmental (a_s) and the normal (a_n) mode as a function of $T - T_g$. For temperatures larger than $T_g + 30$, the shift factors of the two modes are the same within the experimental error. The segmental mode slows down more rapidly when approaching T_g, and at T_g the difference is about a factor of 10. All these results are compatible with literature data.

Many polymeric systems show a temperature dependence of the segmental mode different from that of the normal mode. It is noted that shear compliance measurements on different systems show identical temperature dependence for $T > T_g + 30$ and an increasing difference when approaching T_g with a system dependent magnitude.[17] In the past the different temperature dependence has often been explained in terms of the so-called coupling model (e.g., refs 19 and 20). This model predicts the following relation between the two shift factors: log(a_s) = (β_n/β_s) log(a_n), where β_s is the stretched exponent that characterizes the segmental mode and β_n is the stretched exponent that characterizes the normal mode. Given that $\beta_n > \beta_s$ at least for the lower molar mass samples, the model correctly predicts the existence of different shift factors for the two modes. However, this relation cannot explain the full temperature dependence shown in Figure 4. At high temperatures $a_s = a_n$, implying $\beta_s = \beta_n$, while at low temperatures $a_s > a_n$, implying that β_s/β_n decreases, in contrast with the experimental finding that β_s/β_n is constant over the whole temperature range. In addi-

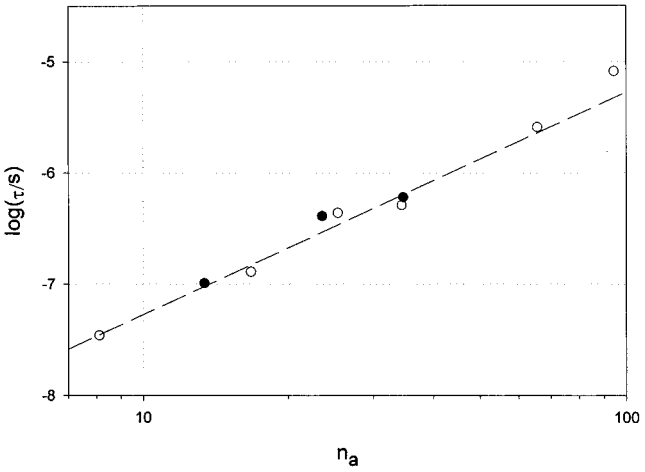

Figure 5. Double logarithmic representation of the dependence of the normal mode obtained at $T = T_g + 130$ K from DS on the number of segments per arm of POP diols (open symbols) and triols (closed symbols). The dashed line has a slope of 2, which represents the prediction of the Rouse model.

tion, the ratio β_s/β_n obtained from DS increases with increasing molar mass while the data in Figure 4 do not show a significant molar mass dependence.

Alternatively, the decoupling of segmental and conformational relaxation has been related to the increasing length scale of dynamic heterogeneity or cooperative motion when approaching T_g. Conformational relaxation on the length scale of the dynamic heterogeneity occurs together with the segmental relaxation. If the length scale of the dynamic heterogeneity equals $\sqrt{\langle r^2 \rangle}$ the characteristic relaxation times merge and all normal modes relax together with the segmental relaxation. This idea has been exploited by Schönhals et al.[1] to estimate the length scale of the segmental relaxation at different temperatures close to and below T_g from the merging temperature of polymers of different sizes. Reasonable values for the length scales were obtained, but it is clear that this estimate is only approximate as the segmental relaxation is broad and is probed differently by different techniques, e.g., the maximum loss of the shear modulus is faster by a factor of 8 (see below).

The molar mass dependence of the normal mode is independent of the distance from T_g and is shown for $T_g + 130$ in Figure 5. For the interpretation of the normal mode observed in DS it is important to realize that POP diols and triols can be considered as stars with two and three arms, respectively. When going from one arm to another the direction of the dipoles is inverted. DS is therefore sensitive only to the fluctuation of the end-to-end vector of an arm. To facilitate comparison between linear and branched samples, the data in Figure 5 are plotted as a function of the number of POP segments per arm, taking the diols as polymers with two arms. The dashed line with slope 2 shows the prediction of the Rouse model. The results of both the diols and triols with less than 50 segments per arm are consistent with this prediction. The deviation at the largest arm length can be attributed to the effect of entanglement (see below).

Schonhals et al.[2] reported a stronger molar mass dependence (M^3) of the normal mode than predicted by the Rouse model based on three linear samples with molar mass between 1000 and 4000 g/L. This observation was interpreted as being the result of entanglements between transient associates caused by hydrogen bonding of end groups. On the basis of the results shown in Figure 5, we believe that this observation was due to an underestimation of the molar mass, especially for the largest sample. In fact, measurements on a sample with the nominal molar mass 4000 synthesized using an older method gave a larger value of the relaxation time close to the value reported by Schönhals et al. The molar masses of T4100 and D3000 are also probably somewhat underestimated. The larger molar mass dependence of the conformational relaxation of the shear modulus reported in ref 16 can be explained in the same way.

II. Shear Modulus. Our aim here is to provide a quantitative comparison of the dielectric and rheology data. In a recent paper shear modulus data on POP diol and triol have been reported.[16] For the present study we have extended those results with measurements on two samples of higher molar mass (D12200 and D8200) and samples D4200 and T6300 with a better defined functionality compared with the earlier used samples of the same nominal molar mass. In the earlier paper it was shown that the shear modulus can be well described using a stretched exponential for the segmental mode and the Rouse model for the normal mode. We cannot access the glassy modes with the apparatus used.

As discussed in ref 16 also in the shear modulus measurements, one observes that the segmental mode has a stronger temperature dependence than the normal mode. However, due to the limited frequency range one can observe both modes only over a narrow temperature range. Within this range, the temperature dependence of the ratio of the shift factors (a_n/a_s) is the same as in DS (see Figure 4).

For the samples with arm molar mass larger than 2000, the Rouse model no longer describes correctly the conformational relaxation due to the effect of entanglement. Therefore we have included in the fit a disentanglement mode in the form of a log-normal distribution of relaxation times. As the effect of entanglement is still small even for D12200, the fit is not sensitive to the exact shape of the distribution, but a single exponential is clearly not sufficient. In Figure 6 are shown master curves of the loss and storage moduli for D12200, which were obtained by superimposing data taken at temperatures higher than the reference temperature in the low-frequency range and data taken at temperatures lower than the reference temperature in the high-frequency range. The solid lines in Figure 6 represent the results of a nonlinear least-squares fit to eq 4 of ref 16 with the addition of the disentanglement mode. The dashed curves show the individual contribution of the segmental mode, the Rouse modes, and the disentanglement mode. The effect of entanglement is also evident for D8200, and even for the samples D4200 and T6300, we can detect small deviations from the Rouse model so that we estimate the arm molar mass where entanglement starts at 2000 g/mol. The mechanical measurements are consistent with the DS measurements, and there is no need to invoke entanglements due to transient hydrogen-bonded intermolecular structures as suggested in ref 13.

The shape of the segmental mode is independent of the molar mass and can be described as a stretched exponential with stretched exponent 0.49; see Figure 1 of ref 16. In Figure 7 the loss dielectric permittivity and shear modulus peaks of the segmental relaxation

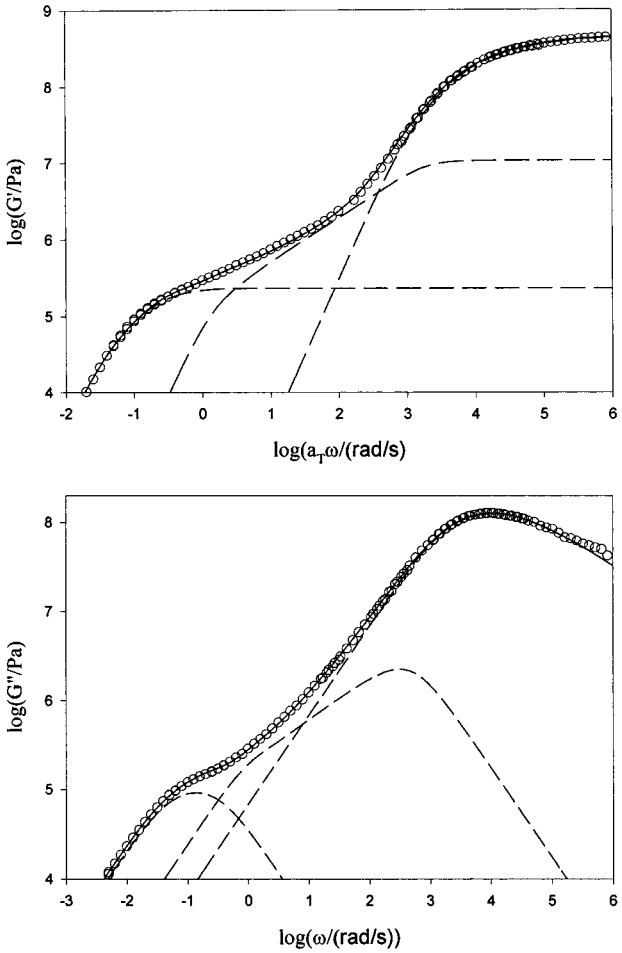

Figure 6. Master curves of the frequency dependence of the storage (top) and loss (bottom) modulus of sample D12200. The master curves were obtained by superimposing data taken at temperatures higher than the reference temperature (218K) in the low-frequency range and data taken at temperatures lower than the reference temperature in the high-frequency range. The solid lines represent fits to a combination of a stretched exponential to describe the high-frequency domain, the Rouse spectrum for the intermediate regime, and a log-normal relaxation time distribution for the low-frequency side (see text). The dashed lines show the individual contributions of each type of relaxation.

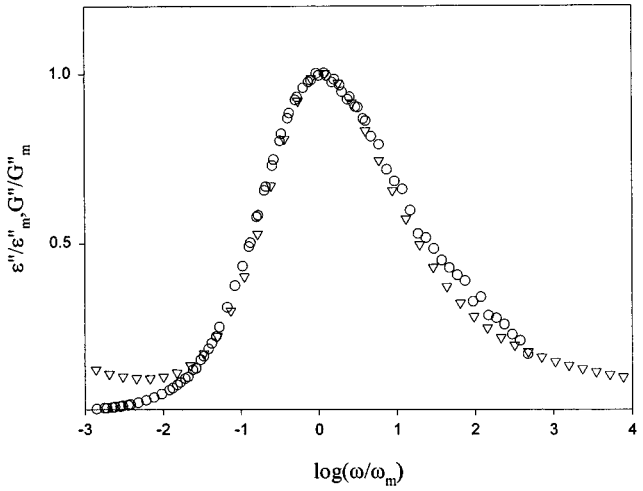

Figure 7. Comparison of the normalized dielectric loss permittivity (triangles) and shear modulus (circles). The DS data are taken at a single temperature $T = T_g + 13$ K, while the mechanical data represent master curves with $T_{ref} = T_g + 13$ K. In this semilogarithmic representation one sees mostly the segmental relaxation although the influence of other modes is visible at low and high frequencies.

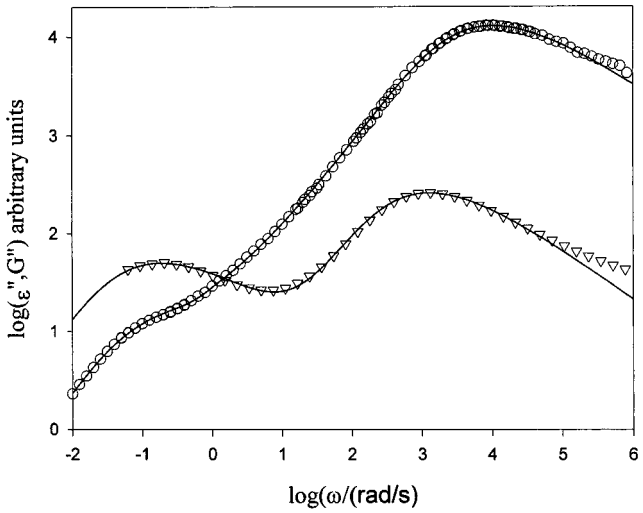

Figure 8. Comparison of the dielectric loss permittivity (triangles) and shear modulus (circles) of sample D12200. The DS data are taken at a single temperature $T = T_g + 13$ K, while the mechanical data represent master curves with $T_{ref} = T_g + 13$ K. The solid lines represent fits to the models discussed in the text.

of D12200 are compared. The loss peak obtained from DS is slightly narrower and this is reflected in the slightly higher stretched exponent. The spectrum of normal modes cannot be directly compared, as the dielectric relaxation is sensitive to fluctuations of the end-to-end vector while shear modulus relaxation is equally sensitive to all Rouse modes. In fact, one cannot discern a loss peak for the conformational relaxation in the shear modulus data even for the largest sample. Figure 8 shows the comparison of the results obtained by dielectric spectroscopy and shear modulus measurements for D12200. The segmental mode obtained from DS is slower, while the normal mode is slightly faster. The DS data shown in Figures 7 and 8 are taken at a single temperature $T = T_g + 13$ K, while the mechanical data represent master curves with $T_{ref} = T_g + 13$ K.

We have taken the characteristic relaxation time of the conformational relaxation of the shear modulus as the slowest Rouse mode for the smaller diols and triols and as the maximum of the log-normal distribution characterizing the disentanglement for the larger samples. The temperature dependence of the segmental and normal modes are compared with those obtained from DS in Figure 9. For clarity we show only the results for two molar masses, but the comparison for all other samples is similar. The segmental relaxation as probed by shear modulus data (τ_{vis}) is systematically faster by a factor of 8 ± 1 than the one measured in dielectric spectroscopy (τ_{DS}), while the conformational relaxation is slower by a factor of 2.5 ± 0.5 (see Table 1). The temperature dependence of both modes can be superimposed by simple vertical shifts and is the same as obtained from DS (see Figure 3b). To obtain exact superposition we have had to assume, in a few cases, slight differences in T_g (at most 1.5 deg) for the DS and the shear modulus data on the same sample.

Within the framework of the Rouse model one expects that the conformational relaxation observed in the shear modulus measurements is slower by a factor of 2 than the relaxation observed in DS for the following reasons. On one hand the relaxation times of the Rouse modes

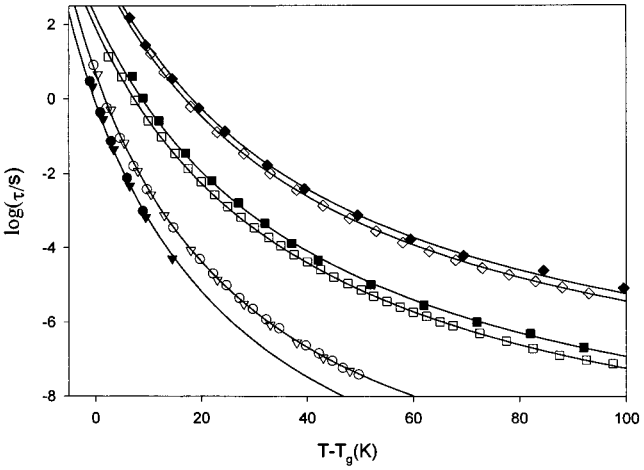

Figure 9. Comparison of the characteristic relaxation times obtained from DS (open symbols) and shear modulus measurements (filled symbols). For clarity we only show the results on D2000 (circles represent the segmental mode, and squares represent the normal mode) and on D12200 (triangles represent the segmental mode, and diamonds represent the normal mode).

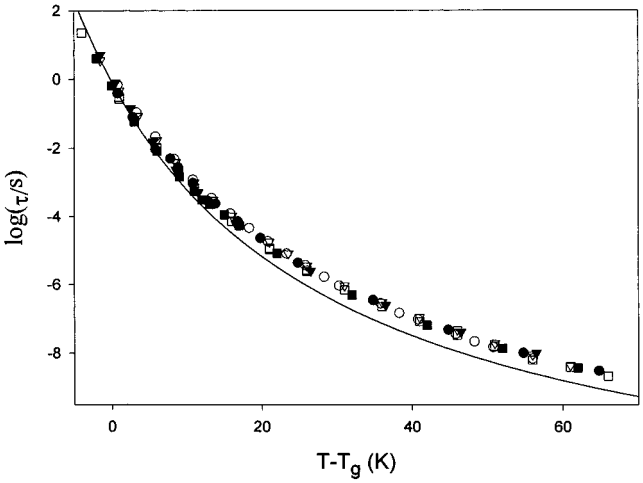

Figure 10. Temperature dependence of the segmental relaxation time of T260 (triangles), T720 (squares), and D425 (circles). The results of DS (open symbols) were shifted upward by about a factor of 8 to coincide with the shear modulus results (filled symbols). The solid line represents the fit of the VFT equation to the results of the high molar mass samples (see Figure 3).

in shear modulus data are 2 times faster than those that characterize fluctuations of the end-to-end vector.[24,25] A comparison of viscoelastic and dielectric relaxation on polyisoprene shows that a difference of about a factor of 2 is observed even for weakly entangled polymers.[25] On the other hand, the slowest motion observed in shear measurements occurs over the length scale of two arms while DS is only sensitive to the motion over the length scale of one arm due to dipole inversion at the center. In other words, the slowest Rouse mode observed in DS is the second mode, which is 4 times faster than the first. The combination of these two effects leads to the expectation that the normal mode observed in shear modulus measurements is slower by a factor 2 than the one observed in DS. The experimental results are compatible with this prediction.

The difference between the segmental relaxation times is not so readily explained, as DS probes the rotational motion of the dipoles, which is not in general related to the shear modulus. However, dynamic light scattering (DLS) measurements on linear POP melts showed that the relaxation times obtained from polarized and depolarized scattered light are the same within experimental error.[9] This implies that rotational and translational motion are strongly coupled. In polarized DLS one measures essentially the relaxation of the longitudinal compliance.[26] Due to the strong coupling of rotational motion and density fluctuations, one expects that the segmental relaxation times observed in DS are close to that of the longitudinal compliance. This would imply that DLS and DS give the same relaxation times for the segmental relaxation. For poly(phenylmethyl siloxane), for which the dipole moment lies on the chain backbone a good agreement was found between DS and DLS,[27] whereas for poly(cyclohexyl methacrylate), with the dipole on the side chain, a disagreement was found.[28] For POP, the observed DLS relaxation times are closer to those obtained by the DS result than those obtained by the shear modulus measurements, although a precise comparison is difficult due to the limited temperature range of the DLS data.

Ultrasonic spectroscopy (US) shows that the relaxation of the longitudinal modulus is close to that of the shear modulus.[29] This means that the faster segmental relaxation of the shear modulus compared to that of the dielectric permittivity can be understood by the fact that the characteristic relaxation time of a modulus is always larger than that of a compliance. The difference depends on the width of the relaxation and the ratio between the high- and low-frequency modulus. Differences between results from US and DLS could be quantitatively explained in this way.[30,31]

III. Finite Size Effects. For smaller samples one can no longer neglect the dielectric signal from the hydroxyl end groups. This is reflected in the increase of the value of $T\Delta\epsilon$, which starts for $M < 4000$ g/mol and becomes very important for the smallest samples: $T\Delta\epsilon = 1650$ for D425 and T720 and 5500 for T260. Nevertheless, one still observes the β-relaxation with the same activation energy and approximately the same values of f_m except for the sample T260, for which f_m is smaller by about a factor 20. In addition, the amplitude of this mode also increases, although not as much as for the segmental mode. This means that one can exclude a specific motion of the POP segments as the origin of the β-relaxation since hydroxyl groups are partially involved in the motion.

The finite size effect on the glass transition temperature of POP triols is peculiar when compared with that of POP diols: for the smallest diol, T_g is lower, while for the smallest triols, T_g is higher. The decrease of T_g of the smallest diol can be rationalized as the usual free-end effect mitigated by hydrogen bonding. The increase of T_g of the smallest triols has to be attributed to the effect of the central propylene glycol core from which the POP chains are grown. The temperature dependence of the segmental relaxation for the smaller samples is compared in Figure 10. For these samples no normal mode is observed and the temperature dependence of the segmental relaxation of the shear modulus can be compared with that obtained from DS over a wide temperature range. In Figure 10 the shear modulus data have been shifted by about a factor of 8 to coincide with the DS data. The temperature dependence of the smaller samples is slightly weaker than that of the high molar mass samples given by the solid line.

As shown in ref 16, the width of the loss shear modulus peak is independent of the molar mass, except in the case of T260 where it was slightly broader. As mentioned above, the width of the loss dielectric permittivity peak decreases slightly with decreasing molar mass. The sample T260 is an exception in the sense that the peak width is not independent of the temperature. This behavior of T260 can be explained by the fact that this sample is in fact a blend of a triol containing three POP segments and a triol containing two POP segments. The existence of concentration fluctuations in blends can lead to a temperature-dependent width.[32]

Conclusion

The main conclusions from the present work are as follows:

1. The molar mass dependence of POP diols and triols displays the classical behavior predicted by the Rouse model ($\tau \propto M^2$) over length scales up to about 80 segments and an effect of entanglements at larger length scales. Also, the frequency dependence of the shear modulus is in quantitative agreement with the Rouse model up to this length scale. The frequency dependence of the dielectric permittivity deviates from the Rouse model.

2. At $T > T_g + 30$ K the temperature dependence of segmental and normal modes is identical, but at $T < T_g + 30$ K the temperature dependence of the segmental mode is steeper. The decoupling of the two modes possibly relates to the existence of dynamic heterogeneity.

3. A quantitative comparison of the relaxation of the shear modulus with that of the dielectric permittivity shows that the segmental relaxation is a factor of 8 ± 1 faster and the conformational relaxation is about a factor of 2.5 ± 0.5 slower. These differences can be explained by considering that the same molecular motions are probed differently by the two techniques.

4. Measurements on low molar mass samples show that the so-called β-relaxation is not related to a specific motion of the POP segments, as for these samples, hydroxyl end groups are involved.

5. A glassy mode slower than the β-relaxation was observed with a higher activation energy. The amplitude of this mode is influenced by the water content and is probably related to the relaxation of residual traces of water.

Acknowledgment. This work was supported by a Greek-French collaborative grant (NHRF-CNRS No. 4454). T.N. acknowledges the hospitality of FORTH.

References and Notes

(1) Schönhals, A.; Schlosser, E. *Phys. Scr.* **1993**, *T49*, 233.
(2) Schlosser, E.; Schönhals, A. *Prog. Colloid Polym. Sci.* **1993**, *91*, 158.
(3) Bauer, M. E.; Stockmayer, W. H. *J. Chem. Phys.* **1965**, *43*, 4319.
(4) Stockmayer, W. H.; Bauer, M. E. *Macromolecules* **1969**, *2*, 647.
(5) Yano, S.; Rabalkar, R. R.; Hunter, S. P.; Wang, C. H.; Boyd, R. H. *J. Polym. Sci., Polym. Phys. Ed.* **1976**, *14*, 1877.
(6) Cochrane, J.; Harrison, G.; Lamb, J.; Phillips, D. W. *Polymer* **1980**, *21*, 837.
(7) Alper, T.; Barlow, A. J.; Gray, R. W. *Polymer* **1976**, *17*, 665.
(8) Huang, Y. Y.; Wang, C. H. *J. Chem. Phys.* **1975**, *62*, 120.
(9) Wang, C. H.; Fytas, G.; Lilge, D.; Dorfmüller, Th. *Macromolecules* **1981**, *16*, 1363.
(10) Duggal, A. R.; Nelson, K. A. *J. Chem. Phys.* **1991**, *12*, 7677.
(11) Borjesson, L.; Stevens, J. R.; Torell, L. M. *Polymer* **1987**, *28*, 1803.
(12) Cosgrove, T.; Griffiths, P. C.; Webster, J. R. P. *Polymer* **1994**, *35*, 140.
(13) Fleischer, G.; Helmstedt, M.; Alig, I. *Polym. Commun.* **1990**, *31*, 409.
(14) Levelut, C.; Scheyer, Y.; Boisier, M.; Pelous, J.; Durand, D.; Emery, J. *J. Phys. Condens. Matter* **1996**, *8*, 941.
(15) Johari, G. P. *Polymer* **1986**, *27*, 866.
(16) Randriantoandro, H.; Nicolai, T. *Macromolecules* **1997**, *30*, 2460.
(17) Plazek, D. J.; Schlosser, E.; Schönhals, A.; Ngai, K. L. *J. Chem. Phys.* **1993**, *98*, 6488.
(18) Schönhals, A. *Macromolecules* **1993**, *26*, 1309.
(19) Ngai, K. L.; Schönhals, A.; Schlosser, E. *Macromolecules* **1992**, *25*, 4915.
(20) Ngai, K. L.; Plazek, D. J.; Deo, S. S. *Macromolecules* **1987**, *20*, 3047.
(21) Fischer, E. W.; Hellman, G. P.; Spiess, H. W.; Horth, F. J.; Ecarius, U.; Wehrl, M. *Macromol. Chem. Suppl.* **1985**, *12*, 189.
(22) Nicolai, T.; Gimel, J. C.; Johnsen, R. *J. Phys. II* **1996**, *6*, 697.
(23) Adachi, K.; Kotaka, T. *Prog. Polym. Sci.* **1993**, *18*, 585.
(24) Strobl, G. *The Physics of Polymers*; Springer-Verlag: Berlin, 1996.
(25) Watanabe, H.; Yao, M.; Osaki, K. *Macromolecules* **1996**, *29*, 97.
(26) Wang, C. H.; Fischer, E. W. *J. Chem. Phys.* **1985**, *82*, 532.
(27) Boese, D.; Momper, B.; Meier, G.; Kremer, F.; Hagenah, J.-U.; Fisher, E. W. *Macromolecules* **1989**, *22*, 4416.
(28) Floudas, G.; Fytas, G.; Fischer, E. W. *Macromolecules* **1991**, *24*, 1955.
(29) Baillif, P. Y.; Tabellout, M.; Emery, J. R. Unpublished results.
(30) Tabellout, M.; Baillif, P. Y.; Randrianantoandro, H.; Litzinger, F.; Emery, J. R.; Nicolai, T.; Durand, D. *Phys. Rev. B* **1995**, *51*, 12295.
(31) Drake, P. W.; Dill, J. F.; Montrose, C. J.; Meister, R. J. *J. Chem. Phys.* **1977**, *67*, 1969.
(32) Zetsche, A.; Fischer, E. W. *Acta Polym.* **1994**, *29*, 168.

MA9714068